



ELSEVIER

Contents lists available at ScienceDirect

Chinese Chemical Letters

journal homepage: [www.elsevier.com/locate/ccllet](http://www.elsevier.com/locate/ccllet)

# Iron single-atom/clusters catalysts derived from iron-rich *Enteromorpha* after urea-saturation for Fenton-like reaction

Yujie Zhang, Siyi Liu, Dongdong Chen, Xing Xu\*

School of Environmental Science and Engineering, Shandong University, Qingdao 266237, China

## ARTICLE INFO

## Article history:

Received 26 February 2023

Revised 23 May 2023

Accepted 7 June 2023

Available online 10 June 2023

## Keywords:

SACs

Iron

Clusters

Fenton-like reaction

*Enteromorpha*

## ABSTRACT

Fabrication of single atom catalysts (SACs) by a green and gentle method is important for their practical Fenton-like use. In this work, a high effective iron-based catalyst was prepared from the iron-rich *Enteromorpha* for NPX degradation via peroxymonosulfate (PMS). Both Fe-SACs and iron-clusters was fabricated from the intrinsic iron element in *Enteromorpha* after the urea saturation. The Fe-SACs/clusters can achieve 100% of NPX oxidation within 20 min with the  $k_{obs}$  of  $0.282 \text{ min}^{-1}$ . Quenching tests indicated that the radical pathways were not dominated in the catalytic systems, and strong electron transfer process can be induced in the Fe-SACs/clusters + PMS system by using the NPX as electron donor and Fe-SACs/clusters/PMS\* complexes as electron acceptor. This result was consistent with the phenomenon observed in the galvanic oxidation system. In addition, the Fe-SACs/clusters was deposited onto the ceramic membrane (CM) by the spraying-crosslinking process to form a Fe-SACs/clusters@CM, which showed an effective and continuous NPX degradation in a heterogeneous PMS system.

© 2023 Published by Elsevier B.V. on behalf of Chinese Chemical Society and Institute of Materia Medica, Chinese Academy of Medical Sciences.

Advanced oxidation process (AOPs) can completely mineralize or decompose most of the refractory organic pollutants in water/wastewater, which has shown a promising application prospect [1,2]. Compared with the traditional AOPs, the novel AOPs based on persulfate (peroxymonosulfate (PMS), and peroxydisulfate (PDS)) activation exhibit the advantages such as long half-life, high redox potential and wide application pH range, which makes the technology stand out in the process of treating refractory organic pollutants [3,4]. Recently, the construction of an efficient heterogeneous catalytic system is the main research direction of PMS oxidation technology. The key is to design heterogeneous catalysts with high activity and stability to activate PMS for wastewater treatment [5,6]. The current research goal is to design low-cost heterogeneous catalysts with good stability and avoid secondary pollution to achieve efficient degradation of pollutants [7–10].

Single atom catalysts (SACs) have extremely high catalytic activity, which can expose the active metal sites to the maximum extent, and break the limitations of traditional catalytic processes on kinetics and catalytic activity, which has become a research hotspot in the field of AOPs [11–13]. Currently, various synthesis strategies (pyrolysis, wet chemical synthesis, physical and chemical vapor deposition, electrochemical deposition, ball milling, etc.) have been used to prepare multifunctional SACs [14–18]. However,

most current preparation processes for SACs are complex and cost sensitive. The primary key to the AOPs-based catalysts is the cost requirement [19–21]. Complex and expensive catalysts are usually not preferred for advanced oxidation applications. As a result, a green and low-cost strategy is required for the fabrication of AOP-based SACs.

As a transition metal, iron is widely found in many biomass materials in nature. Among them, the iron content of *Enteromorpha* is as high as 0.2–0.5 wt%, which is much higher than that of other Marine algae and other biomass materials [22]. *Enteromorpha* is a kind of seasonal Marine pollution algae, can lead to bloom, produce toxic metabolic waste to Marine organisms, consumption of dissolved oxygen, cause great impact on the coastal ecological environment. Especially in Shandong coastal cities, the problem of seasonal pollution of *Enteromorpha* is particularly serious, which has become one of the key points of Marine pollution monitoring and control in recent years. It was found in the previous study that the polysaccharides, proteins and other nitrogen compounds in *Enteromorpha* can coordinate with abundant iron elements in *Enteromorpha* under the condition of high temperature pyrolysis [22]. Without the addition of nitrogen sources and metal precursors, atomic cluster catalysts with a high iron loading capacity of 0.87–1.35 wt% can be prepared [22]. The metal load is comparable to that of most SACs reported so far. Due to the low nitrogen content in *Enteromorpha* and its weak anchoring effect on iron, only ~10% of the iron in *Enteromorpha* was transformed into the dispersed iron atoms, while 90% of the iron elements in *Enteromorpha*

\* Corresponding author.

E-mail address: [xuxing@sdu.edu.cn](mailto:xuxing@sdu.edu.cn) (X. Xu).

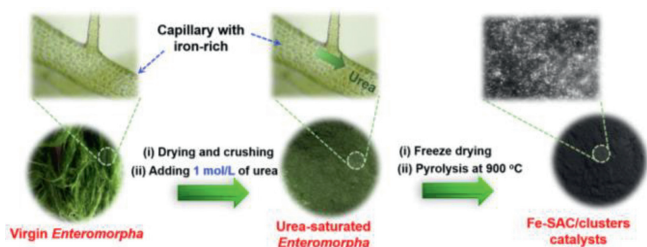


Fig. 1. Preparation scheme of Fe-SAC/clusters catalysts from iron-rich *Enteromorpha*.

gather in the carbon layer structure in the form of iron clusters [22]. Because the SACs mainly relied on the number of dispersed metal atoms to achieve its ultra-high catalytic activity, therefore, how to improve the atomic dispersion of high content iron elements in *Enteromorpha* is the key to achieve the large-scale preparation and efficient application of *Enteromorpha* based Fe-SACs.

In this work, the iron-based catalyst was prepared from the iron-rich *Enteromorpha* which was collected from the Qingdao harbor, Shandong province. The dried *Enteromorpha* was first mixed with 1 mol/L of urea solution for saturating the dried *Enteromorpha* with urea, which could increase the dissolved nitrogen content in the *Enteromorpha* (Fig. 1). The urea-saturated *Enteromorpha* was then freeze dried and pyrolyzed to obtain the iron-based catalyst with improved dispersion of iron atom and reduced amounts of iron-clusters (Fe-SACs/clusters).

The X-ray absorption fine structure (XAFS) can provide the accurate coordination structure in the metal-based catalyst [23–25]. The Fe K-edge X-ray absorption near-edge structure (XANES) spectra of Fe-SACs/clusters catalysts and standard samples was given in Fig. 2a. Result indicated that the state of Fe in the Fe-SACs/clusters was located between Fe(II) and Fe(III). The coordination number of the Fe-SACs in as-prepared catalysts was determined by the Fourier transform-extended X-ray absorption fine structure (FT-EXAFS) spectra (Fig. S2 in Supporting information). The fitting parameters were given in Table S1 (Supporting information) by comparison with the standard samples. Results showed that the coordination number of Fe-SACs in the Fe-SACs/clusters was 3.09, which indicated that the coordination structure in the Fe-SACs was located at Fe-N<sub>3</sub>-C. What is more, the strong Fe-Fe bond in the iron-clusters can also be verified as shown in Table S1. As a result, the FT-EXAFS spectra confirmed the existence of both Fe-SACs and iron-clusters in the as-prepared catalysts. In addition, wavelet transform (WT) contour plots of Fe-SACs/clusters showed an intensity maximum located at ~4.7 Å (Fig. 2b). It can be attributed to the Fe-N coordination. In contrast, the WT of standard Fe foils was located at 7.1 Å

The high angle annular dark field scanning TEM (HAADF-STEM) image of Fe-SACs/clusters derived from 1 mol/L of urea-saturated *Enteromorpha* with microscopic size at 2 nm was given in Fig. 2c.

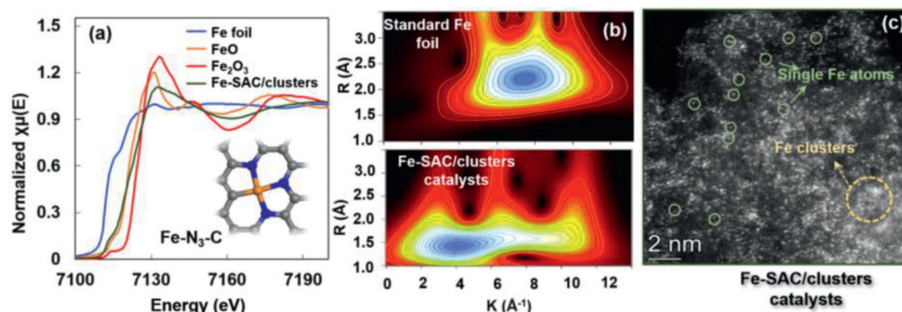


Fig. 2. (a) Fe K-edge XANES spectra of Fe-SACs/clusters catalysts and standard samples (coordination structure of Fe-SACs in as-prepared catalysts was Fe-N<sub>3</sub>-C). (b) WT contour plots of *Enteromorpha*-derived Fe-SACs/clusters catalysts and Fe foils. (c) HAADF-STEM of *Enteromorpha*-derived Fe-SACs/clusters catalysts.

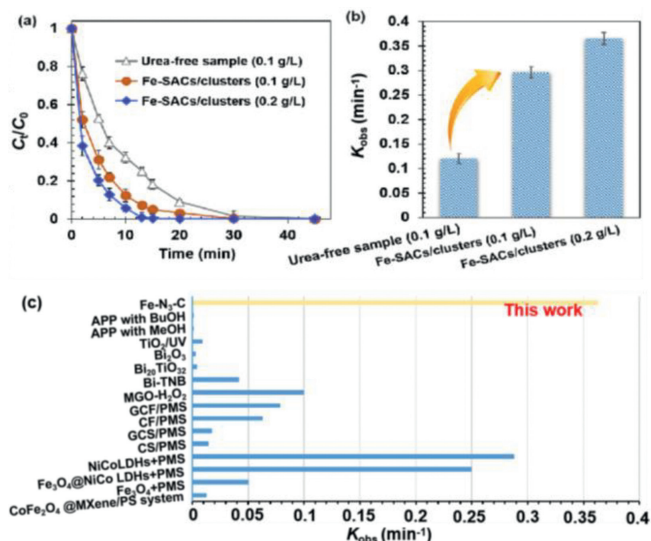
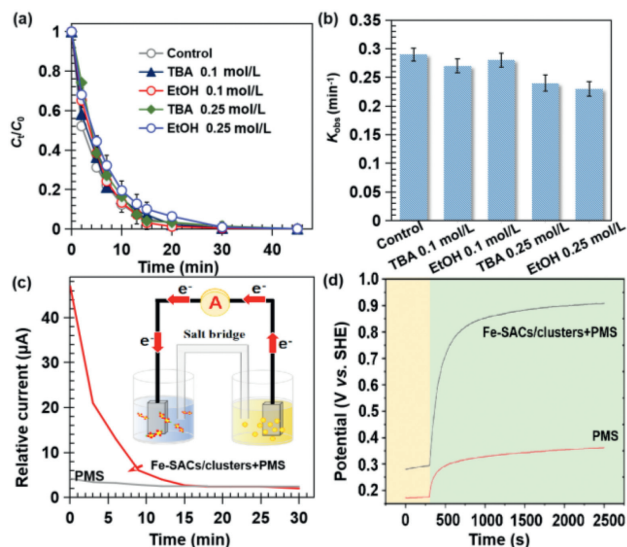


Fig. 3. (a) Degradation of NPX by different *Enteromorpha*-based catalysts. (b)  $K_{obs}$  values of different *Enteromorpha*-based catalysts (10 mg/L of NPX, 0.5 mmol/L of PMS, catalyst dosage: 0.1 g/L). (c) Comparison of catalytic performance with other catalysts.

The results showed that the highly dispersed spots with the minority of aggregated spots can be “visualized”, which indicated that high amounts of Fe-SACs with scattered iron-clusters were fixed onto the carbon matrixes. The dispersion of Fe-SACs has been significantly improved as compared with that of iron-based catalyst prepared from urea-free *Enteromorpha*. As shown in Fig. S2, the iron-based catalyst prepared from urea-free *Enteromorpha* exhibited large aggregated iron-clusters, which confirmed that the 1 mol/L of urea saturation could promote the Fe-N coordination and decrease the Fe-Fe bonds in the urea-saturated *Enteromorpha*, so as to reduce the existence of iron-clusters. As a result, both XAFS and HAADF-STEM measurements could provide the accurate information on the structure of Fe-SACs/clusters.

The degradation of NPX by Fe-SACs/clusters prepared from 1 mol/L of urea-saturated *Enteromorpha*, and urea-free *Enteromorpha* were shown in Figs. 3a and b. The dosage of 0.1 g of Fe-SACs/clusters can achieve 100% of NPX oxidation within 20 min with the  $k_{obs}$  of 0.282 min<sup>-1</sup>. The degradation of NPX was then increased to 0.363 min<sup>-1</sup> by adding 0.2 g/L of Fe-SACs/clusters. In contrast, urea-free sample showed less catalytic performance as compared with that of urea-saturated sample; this indicated that the saturation of urea could improve the iron distribution and therefore promote the catalytic performance [17,25]. Comparison of Fe-SACs/clusters with other catalysts for NPX degradation was shown in Fig. 3c and Table S2 (Supporting information). Re-



**Fig. 4.** (a) Quenching results in the Fe-SAC/clusters+PMS systems; (b)  $K_{obs}$  data in different quenching tests; (c) Relative current of galvanic oxidation system GOS with the Fe-SAC/clusters+PMS systems; (d) Open-circuit potential of Fe-SAC/clusters+PMS system (10 mg/L of NPX, 0.5 mmol/L of PMS, catalyst dosage: 0.1 g/L).

sults showed that the NPX degradation was significantly higher than most reported catalysts and catalytic systems, indicating the exceptional excellent catalytic activity of Fe-SACs/clusters derived from urea-saturated *Enteromorpha*. In addition, the stability of Fe-SACs/clusters was determined, which showed that after still 95% of catalytic capacity can be maintained after 4 cycles (Fig. S3 in Supporting information).

Quenching tests were conducted to confirm the degradation mechanism in the Fe-SACs/clusters+PMS system. TBA was selected as a HO<sup>•</sup> scavenger and EtOH was used as probe for both SO<sub>4</sub><sup>•-</sup> and HO<sup>•</sup> [15,20,22]. As shown in Fig. 4a, the addition of 0.1–0.25 mol/L of TBA and EtOH only showed a very small inhibition on the NPX degradation, with the  $k_{obs}$  decreased from 0.282 min<sup>-1</sup> to 0.233–0.270 min<sup>-1</sup> (Fig. 4b). This result indicated that the radical pathways were not dominated in the catalytic systems. The salt bridge experiment was conducted by putting the PMS and NPX in two separated cells with the Fe-SACs/clusters immobilized onto the graphite electrode, as shown in a galvanic oxidation system (Fig. 4c). A significant current can be observed in the Fe-SACs/clusters immobilized graphite electrode, while no current was shown in the blank graphite electrode (no catalyst was covered). This result indicated that strong electron transfer process was induced by the Fe-SACs/clusters [26].

In addition, open-circuit potential in the Fe-SACs/clusters+PMS system showed a significant increase from 0.3V to 0.9V, which was assigned to the formation of Fe-SACs/clusters/PMS\* complexes (Fig. 4d). In contrast, no significant open-circuit potential can be observed with the absence of Fe-SACs/clusters [22]. As a result, strong electron transfer process can be induced in the Fe-SACs/clusters+PMS system. This result was consistent with the phenomenon observed in the galvanic oxidation system.

We have deposited the Fe-SACs/clusters onto the ceramic membrane (Fe-SACs/clusters@CM). The Fe-SACs/clusters@CM was prepared by the spraying-crosslinking process [26]. Three steps including spray coating, crosslinking, and annealing at 523 K were involved in the fabrication procedures of Fe-SACs/clusters@CM, as shown in Fig. 5a. The hydrophilic result was determined via a contact angle measurement. Results showed that Fe-SACs/clusters@CM only needed a very short time (<0.4s) to fully permeate, which

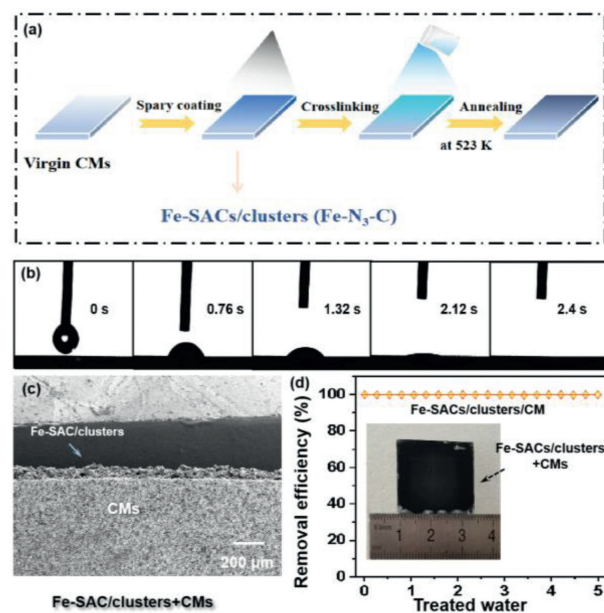


**Fig. 5.** (a) Fabrication procedures of Fe-SACs/clusters@CM. (b) Hydrophilic result of Fe-SACs/clusters@CM. (c) Morphology on the cross-section of Fe-SACs/clusters@CM. (d) Continuous NPX degradation by the Fe-SACs/clusters@CM (1 mg/L of NPX and 0.5 mmol/L of PMS).

indicated that the as-prepared Fe-SACs/clusters@CM had a very good hydrophilicity (Fig. 5b). In addition, the morphology on the cross-section of the Fe-SACs/clusters@CM was also detected, which showed the well-fixed Fe-SACs/clusters on the surface of CM and their thickness was approximately 30 μm (Fig. 5c).

By feeding the Fe-SACs/clusters@CM with 1 mg/L of NPX and 0.5 mmol/L of PMS, we observed that the NPX can be completely removed and the continuous operation test can be maintained for more than 5 L of solution (Fig. 5d). The dosage of Fe-SACs/clusters onto the CM was small (2.0 mg Fe-SACs/clusters /cm<sup>2</sup> of CM), but the well dispersed Fe-SACs/clusters combined with the CM materials could achieve high catalytic performance for the NPX oxidation. This result indicated that the Fe-SACs/clusters@CM could provide a novel strategy for effectively remove the organics in a continuous PMS catalytic system. For future research, the use of the catalyst/CM in a field condition will be important to further evaluate its catalytic activity.

In summary, a high effective iron-based catalyst was prepared from the iron-rich *Enteromorpha* for NPX degradation. Both Fe-SACs and iron-clusters derived from the intrinsic iron element in *Enteromorpha* was fabricated after the urea saturation in the *Enteromorpha*. The electron transfer process was confirmed to be the dominated pathway in the Fe-SACs/clusters+PMS system, while radicals contributed a very minor role for the NPX oxidation. In addition, the depositing of Fe-SACs/clusters onto the CM exhibited a very effective strategy to achieve the continuous NPX degradation in a Fenton-like system.

#### Declaration of competing interest

The authors declare that they have no known competing financial interests or personal relationships that could have appeared to influence the work reported in this paper.

#### Acknowledgments

The work was supported by National Natural Science Foundation of China (No. 52170086), Shandong Provincial Excellent Youth

(No. ZR2022YQ47). The authors also want to thank Conghua Qi from Shiyanjia Lab ([www.shiyanjia.com](http://www.shiyanjia.com)).

### Supplementary materials

Supplementary material associated with this article can be found, in the online version, at [doi:10.1016/j.ccl.2023.108666](https://doi.org/10.1016/j.ccl.2023.108666).

### References

- [1] F. Guo, H. Zhang, H. Li, Z.R. Shen, *Appl. Catal. B* 306 (2022) 121092.
- [2] F. Chen, L. Liu, J. Chen, et al., *Water Res.* 191 (2021) 116799.
- [3] Y. Su, M. Lu, R. Su, et al., *Chin. Chem. Lett.* 33 (2022) 2573–2578.
- [4] Q. Zhao, C.C. Wang, P. Wang, *Chin. Chem. Lett.* 33 (2022) 4828–4833.
- [5] L. Chen, S. Wang, Z. Yang, J. Qian, B. Pan, *Appl. Catal. B* 292 (2021) 120193.
- [6] X. Hu, D. Zhou, H. Wang, et al., *Chin. Chem. Lett.* 34 (2023) 108050.
- [7] C.A. Akinremi, S. Rashid, P.D. Upreti, G.T. Chi, K. Huddersman, *RSC Adv.* 10 (2020) 12941–12952.
- [8] Q. Liu, H. Li, H. Zhang, Z.R. Shen, H.M. Ji, *Chin. Chem. Lett.* 33 (2022) 4756–4760.
- [9] A.A. Oladipo, A.O. Ifebajo, M. Gazi, *Appl. Catal. B* 243 (2019) 243–252.
- [10] X. Wang, J. Jing, M. Zhou, R. Dewil, *Chin. Chem. Lett.* 34 (2023) 107621.
- [11] L. Chen, C. He, R. Wang, et al., *Chin. Chem. Lett.* 32 (2021) 53–56.
- [12] H.L. Fei, J.C. Dong, et al., *Chem. Soc. Rev.* 48 (2019) 5207–5241.
- [13] M.A. Oturan, J.J. Aaron, *Crit. Rev. Environ. Sci. Technol.* 44 (2014) 2577–2641.
- [14] L. Jiao, H. Jiang, *Chem* 5 (2019) 786–804.
- [15] Y.N. Shang, X. Xu, Q.Y. Yue, et al., *Environ. Sci.* 7 (2020) 1444–1453.
- [16] X. Li, L. Liu, X. Ren, et al., *Sci. Adv.* 6 (2020) eabb6833.
- [17] F. Chen, L.L. Liu, J.H. Wu, et al., *Adv. Mater.* 34 (2022) 2202891.
- [18] H. Yang, L. Shang, Q. Zhang, et al., *Nat. Commun.* 10 (2019) 4585.
- [19] H.B. Yang, S.F. Hung, S. Liu, et al., *Nat. Energy* 3 (2018) 140–147.
- [20] Y. Gao, X.G. Duan, B. Li, et al., *J. Mater. Chem. A* 9 (2021) 14793–14805.
- [21] K. Qian, H. Chen, W. Li, et al., *Environ. Sci. Technol.* 55 (2021) 7034–7043.
- [22] L. Peng, X. Duan, Y. Shang, B. Gao, X. Xu, *Appl. Catal. B* 287 (2021) 119963.
- [23] X. Fu, P. Zamani, J.Y. Choi, et al., *Adv. Mater.* 29 (2017) 1604456.
- [24] X. Zhang, S. Zhang, Y. Yang, et al., *Adv. Mater.* 32 (2020) 1906905.
- [25] Y.N. Shang, X. Xu, B.Y. Gao, S.B. Wang, X.G. Duan, *Chem. Soc. Rev.* 50 (2021) 5281–5322.
- [26] P.J. Duan, X. Xu, K.Y. Guo, Q.Y. Yue, B.Y. Gao, *Appl. Catal. B* 316 (2022) 121695.